3-D analytical migration velocity analysis II: Velocity gradient estimation

Zhaobo Meng,* Norman Bleistein† and Paul A. Valasek‡

* *Center for Wave Phenomena, Colorado School of Mines; now Phillips Petroleum Company*
† *Center for Wave Phenomena, Colorado School of Mines*
‡ *Phillips Petroleum Company*

ABSTRACT

We parameterize the reflector-normal misfit (in a common image gather) in different migration parameters. The analytical migration velocity analysis (AMVA) is then treated as a parameter identification problem. We introduce the *reflector-normal directional derivatives*, which connect the measured misfit data with the perturbations to the parameters.

The velocity gradient estimation problem is typically *insufficiently* constrained by the measured misfit data alone. However, the problem may turn into a well-behaved system if other velocity constraints can be incorporated into the system to constrain the uncertainties. Here, we derive a linear system for velocity gradient estimation in such a way that different constraints can be efficiently incorporated into the system.

To test the approach, the proposed algorithms are applied to both a 3-D synthetic data set and a 3-D streamer data set acquired in the Gulf of Mexico. It is found that, although the measured misfit data alone are not sufficient to constrain the uncertainties, there are "enough" other constraints in both cases such that the vertical velocity gradient is resolved within acceptable precision.

Introduction

This paper can be viewed as a continuation of Meng *et al.* (1999), where two-step reflector-normal velocity estimation is studied. Here, we expand the representation of the reflector-normal misfit in common image gathers (CIG) to include the velocity gradients. Velocity gradients are to be estimated from the *governing equations* with the *measured differences in reflector-normal misfits* as input, plus additional velocity constraints. Mathematically, the *governing* equations are based on—and are thus exact for—a (layered) constant gradient background model with arbitrary reflecting subsurface. We adopt a horizon-based imaging (Wyatt, 1995) for estimating the velocity gradients.

The proposed velocity gradient estimation algorithms are tested on both a 3-D land synthetic data set and the 3-D Mahogany streamer data set acquired in the Gulf of Mexico. It is found that the misfit data alone are *insufficient* to determine the velocity gradients; other velocity constraints must be incorporated into the system to constrain the uncertainties. With such supplemental velocity constraints, velocity gradients are resolved within reasonable precision in both data tests. Here, we employ only sufficient constraint to estimate the vertical component of the velocity gradient and those are the results that we describe here.

The system for velocity gradient estimation

With details in the Appendix, a linear system of differential equations are developed for the velocity gradient estimation. In this system, the governing equations for the velocity gradient estimation are written as

$$2\delta L = -\Delta z\left(\tilde{g}_1\frac{\partial}{\partial x}+\tilde{g}_2\frac{\partial}{\partial y}\right)\delta v_z+$$

$$(\Delta z\tilde{g}_0+(n_1^0+n_1^1)\tilde{g}_1+(n_2^0+n_2^1)\tilde{g}_2-2\tilde{g}_3)\delta v_z. \qquad (1)$$

Here, $\tilde{g}_k(\gamma,h)$, $k=0,1,2,3$ are the differences in the reflector-normal directional derivatives introduced in the Appendix; γ is the azimuth and h is the half-offset. Furthermore, the two dimensionless quantities

$$n_1^0(x,y) \equiv \frac{\partial}{\partial x} z_0(x,y), \qquad n_2^0(x,y) \equiv \frac{\partial}{\partial y} z_0(x,y),$$

are the horizontal components of the normal vector, ∇z_0, to the top horizon, $z = z_0(x,y)$ and

$$n_1^1(x,y) \equiv \frac{\partial}{\partial x} z_1(x,y), \qquad n_2^1(x,y) \equiv \frac{\partial}{\partial y} z_1(x,y),$$

are the horizontal components of the vector normal to the base horizon, $z = z_1(x,y)$. Finally,

$$\Delta z(x,y) \equiv z_1(x,y) - z_0(x,y),$$

is the vertical thickness of the target layer.

As in Meng *et al.* (1999), $\delta L(\gamma, h)$, in equation (1) is called the *differences in reflector-normal misfits*. $\delta L(\gamma, h)$ is the difference between the imaged point, $\mathbf{x}(\gamma, h)$, and $\mathbf{x}(\gamma, 0)$, projected on the reflector-normal direction, $\mathbf{n}$. In practice, an automatic search algorithm can be used to "pick" the differences in reflector-normal misfits, $\delta L(\gamma, h)$. In addition, the differences in the reflector-normal directional derivatives, $\tilde{g}_k$'s, can be evaluated analytically by using the migration model parameters, which will be discussed in the Appendix.

Other information, velocity constraints (A33), (A38) and (A39), as well as well logs, can be incorporated into the linear system, as well.

In addition, the discrete system of the above linear equations of (1), (A33), (A38) and (A39), is extremely sparse. For 3-D, without the use of a sparse linear equation solver, the memory- and computation-cost of solving such a large linear system may be prohibitive. The conjugate gradient method, though, allows efficient sparse matrix processing that reduces this cost and has been tested for both synthetic and field data examples (Scales, 1987).

¿From a theoretical point of view, the differences in the reflection-normal directional derivatives, $\tilde{g}_0$, $\tilde{g}_1$, $\tilde{g}_2$ and $\tilde{g}_3$, are an indicator of when a gradient estimation is necessary. Small values in $\tilde{g}_k$'s indicate that a stationary point in the parameter plane (or a local minimum) is reached; thus a further gradient perturbation at this point should be avoided. On the other hand, large g_k's may suggest that a gradient perturbation search is necessary.

Velocity gradient estimation for a 3-D synthetic land data set

To test the proposed velocity gradient estimation algorithms as restricted to v_z estimation only, a 3-D synthetic data set is used. The same dataset was used for test on the two-step velocity estimation and is reported in Meng *et al.* (1999), with Figure 1 in Meng *et al.* (1999) showing the true model.

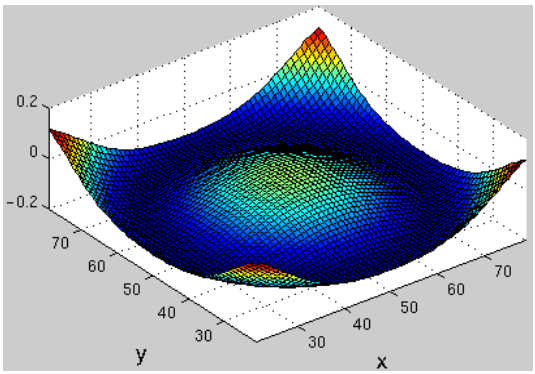

Figure 1. The true vertical velocity gradient in the imaging area. The vertical velocity gradient equals zero at the center, then decreases to $-0.13/s$ midway before increasing to $0.13/s$ at the corners of the model.

After several iterations of the two-step velocity estimation, it is assumed that the top horizon velocity is close to the true velocity in the target layer.

Following the horizon-based prestack depth migration (HPSDM) (Wyatt, 1995), the reflector-normal directional derivatives, g_k's, are computed at different offsets, including at zero offset. These measurements give the terms, $-\tilde{g}_k(\gamma, h)$, in equation (1) or (A32). In addition, the differences in reflector-normal misfits, $\delta L(\gamma, h)$, are picked at the same offsets and azimuths. Thus, all quantities in linear system (1) or (A32) are known, except for the perturbations to parameters, $\delta\lambda_k$. This linear system is solved by a conjugate gradient solver (Scales, 1987).

Figure 1 shows the true vertical velocity gradient, $v_z(x,y)$, in the target layer. Figure 2 shows the estimated vertical velocity gradient, $v_z^1(x,y)$. Figure 3 shows the error of this estimate. The relative error between the estimated vertical velocity gradient, $v_z^1(x,y)$ (Figure 2), and the true value, $v_z(x,y)$ (Figure 1), is typically less than 10%, except at the center, where errors are as high as 25%, due to the geometrical complexity (see Figure 1 in Meng *et al.* (1999)). The vertical velocity gradient estimation algorithm also gives an additional velocity update. Figure 4 shows the velocity, $v_0(x,y)$, at the top horizon of the target layer. Figure 5 shows the error in the velocity, $v_0^4(x,y) - v_0(x,y)$. After the top horizon velocity, $v_0(x,y)$, and its vertical gradient are updated, the base horizon is adjusted by using the base adjustment algorithm introduced in Meng *et al.* (1999). Figure 6 shows a profile view of the center slice in y (iy=50, ix and iy are the node numbers) of the model after the velocity gradient estimation. The estimated top horizon velocity, the vertical velocity gradient and base horizon of the target layer reasonably matches the true parameters in the target layer.

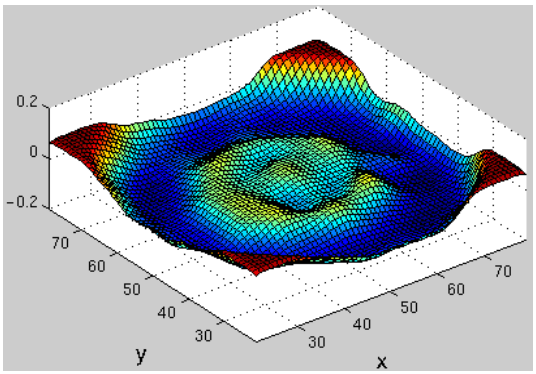

Figure 2. The estimated vertical velocity gradient, $v_z^1(x,y)$. The estimated vertical velocity gradient follows the trend of its true value (compared to Figure 3 in Meng *et al.* (1999)).

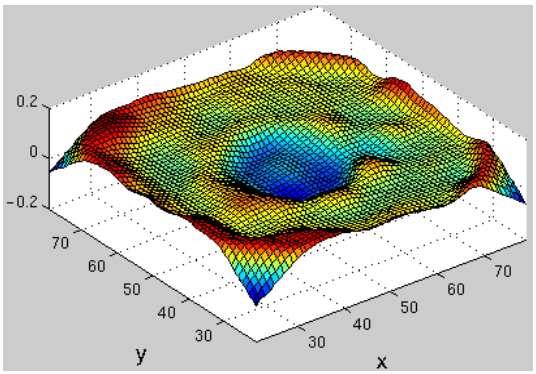

Figure 3. The error in the vertical velocity gradient, $v_z^1(x,y) - v_z(x,y)$. Except at the boundary where there are not enough data, errors in most areas are within 10%. However, errors at the center are up to 25% due to the complexity in the structure.

Velocity gradient estimation for the Mahogany 3-D streamer data set

In the Gulf of Mexico, velocities typically vary as a function of depth of burial. In this situation, it is appropriate to approximate a number of sequential layers, into a single mega-layer with appropriate vertical velocity gradients. Here, we test how this approach works for vertical velocity gradient estimation. Figure 7 shows a profile view of the first five layers of the Mahogany model. In general, linearity in velocities in the first four sediment layers (layer two through layer five) above salt may be a good assumption. To test this idea, layer two through layer five (sediments above salt) of Mahogany model are approximated as a "mega-layer." Vertical velocity gradient estimation is then applied to this mega-layer.

Before vertical velocity gradient estimation, two-step reflector-normal update (Meng *et al.*, 1999) is applied to provide an "averaged" top horizon velocity,

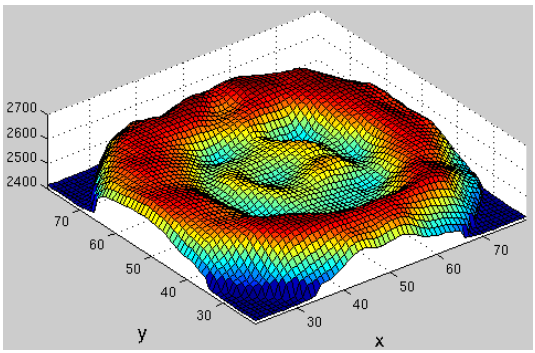

Figure 4. The estimated top horizon velocity, $v_0^4(x,y)$, at the top horizon of layer two after the velocity gradient estimation.

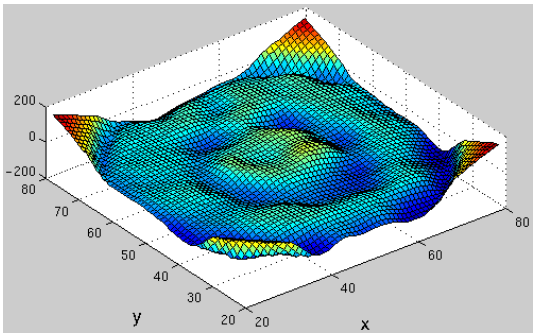

Figure 5. The error in the velocity, $v_0^4(x,y) - v_0(x,y)$, at the top horizon of layer two. Larger errors are seen at the corners due to the lack of data, and some at the center due to the complexity in the structure.

$\overline{v}_0(x,y)$, and depth of the base, $z_1(x,y)$ of the mega-layer. To apply the vertical velocity gradient estimation, HPSDM (Wyatt, 1995) is applied and reflector-normal misfits are picked. Solving the linear system (1) or (A32) using a regularization technique, the top horizon velocity, $v_0(x,y)$, and vertical velocity gradient, $v_z(x,y)$, are estimated.

After vertical velocity gradient estimation, it is often necessary to apply another iteration of two-step velocity estimation (Meng *et al.*, 1999) to the model with the new gradient and the new top horizon velocity. Figure 8 shows a profile view of the final model after the vertical velocity gradient estimation. This model gives satisfactory CIG alignment and is regarded as a model that fits the available well data with acceptable precision.

Conclusions

Based on the analysis of the reflector-normal misfit with respect to the velocity parameters in the target layer, velocity gradient estimation algorithms have been derived, for a solution to a parameter identification problem. Ve-

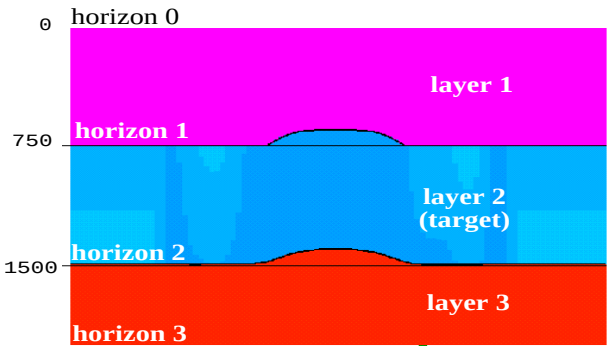

Figure 6. A profile view of the center slice in y (iy=50) of the model after the vertical velocity gradient estimation. One can see that the base horizon (horizon two), $z_1^4(x,y)$, has been well reconstructed. The vertical velocity gradient, $v_z^1(x,y)$, has been resolved with a relative error about 10% at the center area and up to 30% at the boundaries.

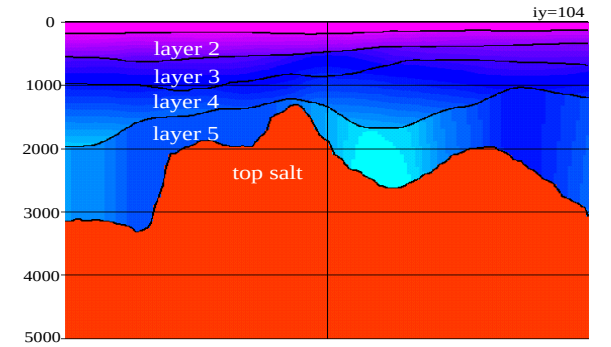

Figure 7. The velocity model obtained by traditional velocity estimation. Some linearity in velocity is observed from layer two to layer five. These four layers will be approximated as a "mega-layer", and a vertical velocity gradient estimation will be applied to this "mega-layer" in this section.

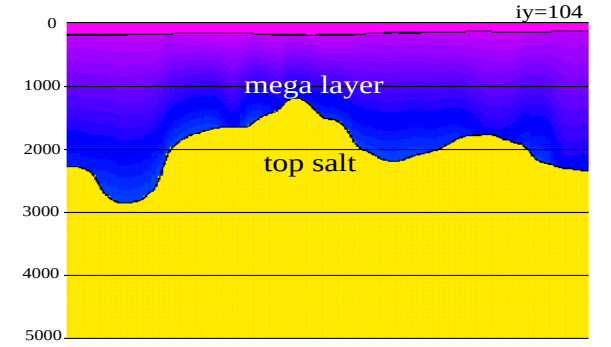

Figure 8. A profile view of the final model obtained after the velocity gradient estimation.

locity gradients are typically *insufficiently* constrained by the measured misfit data. However, the gradient estimation algorithms are derived in such a manner that various constraints can be efficiently incorporated into the system. Velocity gradient estimation algorithms proposed in this paper are designed to be applied after velocity estimation (Meng *et al.*, 1999) when an initial guess for the vertically averaged velocity is found.

To test the velocity gradient estimation, the proposed algorithms have been applied to both a 3-D land synthetic data set and a 3-D streamer data set acquired in the Gulf of Mexico. In both cases, we found enough constraints to help resolve the vertical velocity gradients with *reasonable* precision.

It is important to understand that there is an error bar associated with each parameter. These error bars depend on factors such as the quality of the data, sensitivity of the parameter to the data, the processing procedure, etc. When we stated that the velocities and/or velocity gradients have been "resolved," we meant that they have been resolved with some error bar associated with the velocity/depth/gradient tradeoff. For real data, in general, one cannot be sure these error bars are small enough without additional constraints. Since the noise level in real data is much higher than in synthetic data, it is possible that the singular values corresponding to the noise in the data are greater than the singular values related to velocity/depth/gradient tradeoff. Careful study of velocity/depth/gradient tradeoff has not been carried out in this paper. However, a similar case in the velocity/depth tradeoff was studied by Meng & Bleistein (1999).

Acknowledgments

We are thankful for the numerous comments and advice from Kay Wyatt, Bob Heaton, Jennifer Swanson, Yunqing Shen, Brian K. Macy of Phillips Petroleum Company. The authors greatly acknowledge the financial support by Phillips and by the Office of Naval Research, through CWP, as well as the partial support by the sponsors of the Consortium Project on Seismic Inverse Methods for Complex Structures at the Center for Wave Phenomena, Colorado School of Mines. Finally, we acknowledge the permission from the Geco-Prakla partnership to use the Mahogany, Gulf of Mexico, dataset and to publish the results.

References

Bleistein, N. 1984. *Mathematical Methods for Wave Phenomena.* San Diego: Academic Press.

Cervény, V. 1987. Raytracing algorithms in three-dimensional laterally varying layered structures. *Nolet, G., Ed., Seismic Tomography*, 99–133.

Liu, Z. 1995. Migration velocity analysis. *Pages 1–88 of: Ph. D. thesis, Colorado School of Mines.*

Liu, Z. 1997. An analytical approach to migration velocity analysis. *Geophysics*, **62**, 1238–1249.

Liu, Z., & Bleistein, N. 1995. Migration velocity analysis: Theory and an iterative algorithm. *Geophysics*, **60**, 142–153.

Meng, Z. 1999. Tetrahedral Based Earth Models, Ray Tracing in Tetrahedral Models and Analytical Migration Velocity Analysis. *Pages 1–180 of: Ph. D. thesis, Colorado School of Mines, CWP-296.*

Meng, Z., & Bleistein, N. 1999. On Velocity/Depth Ambiguity in 3-D migration velocity analysis. *This report.*

Meng, Z., Bleistein, N., & Wyatt, K. D. 1999. 3-D Analytical Migration Velocity Analysis I: Two-step Velocity Estimation by Reflector-normal Update. *This report.*

Scales, J. 1987. Tomographic inversion via the conjugate gradient method. *Geophysics*, **52**, 179–185.

Scales, J. 1989. On the use of conjugate gradient to calculate the eigenvalues and singular values of large, sparse matrices. *Geopysical Journal*, **97**, 179–183.

Wyatt, K. D. et. al. 1995. Rapid velocity estimation using horizon-based 3-D prestack depth migration. *In: Research workshop: "Velocity Estimation for 3-D Imaging", 65th Annual Internat. Mtg., Soc. Expl. Geophys*, vol. 65.

APPENDIX A: Parameterization of the reflector-normal misfits

In Meng *et al.* (1999), the idea of perturbations of the imaged point in the reflector-normal direction was introduced, and a reflector-normal velocity update procedure was derived. Here, we extend the parameterization of the velocity in the target layer to include the velocity gradients, and linearize the reflector-normal misfit with the velocity parameters. Following Liu (1995; 1997) and Meng (1999), suppose that the velocity field $v(\mathbf{x})$ is characterized by a parameter or a family of parameters, $\boldsymbol{\lambda}$, in the target layer as $v = v(\mathbf{x};\boldsymbol{\lambda})$. For example, when $v(\mathbf{x};\boldsymbol{\lambda}) = v_0 + ax + by + cz$, $\boldsymbol{\lambda}$ is any set of one to four parameters chosen from v_0, a, b and c. Thus, the velocity gradient estimation becomes a parameter estimation problem (Liu & Bleistein, 1995).

Let us differentiate the imaged point, $\mathbf{x}$, in the post-migration domain, with respect to $\boldsymbol{\lambda} = (\lambda_0, \lambda_1, \lambda_2, \lambda_3)$. Notice that the imaged point, $\mathbf{x} = (x_1, x_2, x_3)$, and surface parameter, $\boldsymbol{\xi}$, (Meng *et al.*, 1999) are all functions of $\boldsymbol{\lambda}$; following Meng (1999), the directional derivatives at the imaged point, $\mathbf{x}$, with respect to the velocity parameter, λ_k, in the reflector-normal direction, $\mathbf{n} = (n_1, n_2, n_3)$, are given by

$$n_j \frac{dx_j}{d\lambda_k} = g_k(\mathbf{x}, \gamma, h), \quad k = 0, 1, 2, 3, \tag{A1}$$

where the *reflector-normal directional derivatives*, $g_k(\mathbf{x}, \gamma, h)$, are given by

$$g_k(\mathbf{x}, \gamma, h) = -\left(\frac{\partial \tau_s}{\partial \lambda_k} + \frac{\partial \tau_g}{\partial \lambda_k}\right) \frac{v(\mathbf{x};\boldsymbol{\lambda})}{2\cos\theta}, \quad k = 0, 1, 2, 3. \tag{A2}$$

Here, θ is the half-opening angle at the imaged point $\mathbf{x}$ (Fig. A1); τ_s and τ_g are the traveltimes from the imaged point, $\mathbf{x}$, to the source, $\mathbf{s}$, and to the receiver, $\mathbf{r}$, respectively. The reflector-normal directional derivatives, $g_k(\mathbf{x}, \gamma, h)$, $k = 0, 1, 2, 3$, govern the relationship between the reflector-normal misfits and the perturbation to velocity parameters, $\delta\lambda_k$, in the target layer.

Suppose that in the target layer, the true velocity parameter is $\boldsymbol{\lambda}^* = (\lambda_0^*, \lambda_1^*, \lambda_2^*, \lambda_3^*)$ and the true reflector is at $\mathbf{x}^* = (x_1^*, x_2^*, x_3^*)$. According to Meng *et al.* (1999), if there is a small perturbation to the velocity parameters, between the true velocity parameters and the parameters used in migration, $\delta\boldsymbol{\lambda} = (\delta\lambda_0, \delta\lambda_1, \delta\lambda_2, \delta\lambda_3) = \boldsymbol{\lambda}^* - \boldsymbol{\lambda}$, then the imaged point, $\mathbf{x}$, will have a corresponding perturbation, $\delta\mathbf{x}$, in the reflector-normal direction, $\mathbf{n}$, which is represented as

$$n_j \delta x_j(\gamma, h) \equiv n_j(x_j^* - x_j(\gamma, h)) \approx n_j \frac{dx_j}{d\lambda_k}\delta\lambda_k. \tag{A3}$$

By using equation (A1), a linearized equation is deduced for the velocity parameter perturbations, $\delta\lambda_k$:

$$n_j(x_j^* - x_j(\gamma, h)) = g_k(\gamma, h)\delta\lambda_k. \tag{A4}$$

Notice that, equation (A4) is valid for a *general* background models, it holds as long as the perturbation to the velocity parameters are small enough.

In equation (A3) or (A4), both the velocity parameter perturbations $\delta\lambda_k$'s, and the true reflector, $\mathbf{x}^* = (x_1^*, x_2^*, x_3^*)$, are unknown. We can avoid this problem using a traditional perturbation strategy (Bleistein, 1984). This is achieved by first introducing the zero-offset imaged point, $\widehat{\mathbf{x}}$, as

$$\widehat{x}_j \equiv x_j(\gamma, 0), \tag{A5}$$

and the zero-offset reflector-normal directional derivatives

$$\widehat{g}_k \equiv g_k(\gamma, 0), \quad k = 0, 1, 2, 3. \tag{A6}$$

Here, we have used $\widehat{\ }$ to denote the zero-offset quantities. Recall hat for zero-offset, azimuth γ does not matter.

Here, we differ from Liu (1995), who used the *averaged imaged point* as a substitute for $\widehat{x}_j$ to apply an operation similar to the following.

Since (A4) holds for all half offset h, it also holds for zero-offset, thus

$$n_j(x_j^* - \widehat{x}_j) = \widehat{g}_k \delta\lambda_k. \tag{A7}$$

Subtracting equation (A4) from equation (A7) eliminates $\mathbf{x}^*$ and yields the *governing equations*

$$\delta L(\gamma, h) \equiv n_j(x_j(\gamma, h) - \widehat{x}_j) = -\tilde{g}_k(\gamma, h)\delta\lambda_k. \tag{A8}$$

Here, we have denoted

$$\tilde{g}_k(\gamma, h) \equiv g_k(\gamma, h) - \widehat{g}_k, \quad k = 0, 1, 2, 3. \tag{A9}$$

Up to this point, the only unknowns in equation (A8) are the velocity parameter perturbations, $\delta\lambda_k$'s. Velocity gradient estimation is basically based on the solution to the governing equations (A8).

Analytical evaluation of the reflector-normal directional derivatives, g_k's

To solve the governing equations for the velocity gradients, the reflector-normal directional derivatives, g_k's need to be evaluated. For speed and accuracy, an analytical evaluation of the g_k's is proposed. Here, the discussion is limited to layered constant gradient background models, with an arbitrary reflecting subsurface.

As is well-known (Cervény, 1987), the ray path in a constant gradient medium is a circle lying in the plane determined by the velocity gradient vector and the (initial) ray vector.

Suppose that the velocity at an imaged point, $\mathbf{x}$, is v_0, at the source, $\mathbf{x}_s = (x_1^s, x_2^s, x_3^s)$, it is v_{0s}, and at the receiver, $\mathbf{x}_g = (x_1^g, x_2^g, x_3^g)$, is v_{0g}. Also, suppose that the gradient of the velocity is the vector $\mathbf{w} = (w_1, w_2, w_3) = \nabla v$. That is, the velocities at the source and receiver, v_{0s} and v_{0g}, are represented as

$$v_{0s} = v_0 + (\mathbf{x}_s - \mathbf{x}) \cdot \mathbf{w}, \tag{A10}$$

$$v_{0g} = v_0 + (\mathbf{x}_g - \mathbf{x}) \cdot \mathbf{w}, \tag{A11}$$

respectively.

Suppose that $\mathbf{p}_s = (p_{1s}, p_{2s}, p_{3s})$ is the (initial) ray vector at $\mathbf{x}_s$, then the norm of the ray vector, $\mathbf{p}_s$, is equal to the slowness. That is,

$$p_{1s}^2 + p_{2s}^2 + p_{3s}^2 = \frac{1}{v_{0s}^2}. \tag{A12}$$

Following Cervény (1987), we introduce a local coordinate system, with origin at the source, $\mathbf{x}_s$, and the three unit axis vectors $\mathbf{e}_1^s, \mathbf{e}_2^s$ and $\mathbf{e}_3^s$ chosen, such that

$$\mathbf{e}_3^s = \mathbf{w}/w, \tag{A13}$$

here, the scalar w is the magnitude of the gradient, i.e., $w = \mid \mathbf{w} \mid$; if the ray vector, $\mathbf{p}_s$, is non-collinear with $\mathbf{e}_3^s$, then choose $\mathbf{e}_1^s$ and $\mathbf{e}_2^s$, such that

$$\mathbf{e}_1^s = \frac{\mathbf{p}_s - (\mathbf{p}_s \cdot \mathbf{e}_3^s)\mathbf{e}_3^s}{\mid \mathbf{p}_s - (\mathbf{p}_s \cdot \mathbf{e}_3^s)\mathbf{e}_3^s \mid}, \tag{A14}$$

$$\mathbf{e}_2^s = \frac{\mathbf{p}_s \times \mathbf{e}_3^s}{\mid \mathbf{p}_s \times \mathbf{e}_3^s \mid}. \tag{A15}$$

Otherwise, i.e. in case $\mathbf{p}_s \parallel \mathbf{e}_3^s$, just choose $\mathbf{e}_1^s$ and $\mathbf{e}_2^s$ arbitrarily such that $\mathbf{e}_1^s$, $\mathbf{e}_2^s$ and $\mathbf{e}_3^s$ are two-two orthonormal. Notice that, in this last case, $\mathbf{e}_1^s$ and $\mathbf{e}_2^s$ are non-unique, but this non-uniqueness does not matter for the analysis. In this last case, the ray path is straight and along $\mathbf{w}$ (or $\mathbf{e}_3^s$). In all cases, according to Cervény (1987), the ray stays within the $\mathbf{e}_1^s$, $\mathbf{e}_3^s$ plane. Now, for clarity, I add a $'$ to denote the quantities represented in the local coordinate system. Thus, now, the velocity gradient can be expressed as

$$\mathbf{w}' = (0, 0, w), \tag{A16}$$

in the new coordinate system. The initial ray vector from the source, $\mathbf{x}_s$, to the imaged point, $\mathbf{x}$, in the new coordinate system is written as

$$\mathbf{p}_s' = (p_{1s}', 0, p_{3s}'), \tag{A17}$$

where the norm of the ray vector in the new local coordinates is not changed,

$$p_{1s}'^2 + p_{3s}'^2 = \frac{1}{v_{0s}^2}, \tag{A18}$$

since the out-of-plane component $p_{2s}' = 0$. The source, $\mathbf{x}_s$, now becomes the origin

$$\mathbf{x}_s' = (0, 0, 0), \tag{A19}$$

and the imaged point, $\mathbf{x}$, in the "source" local coordinate system, denoted as $\mathbf{x}_{Is}'$, becomes

$$\mathbf{x}_{Is}' = (x_{1s}', x_{2s}', x_{3s}') = ((\mathbf{x}-\mathbf{x}_s)\cdot\mathbf{e}_1^s, 0, (\mathbf{x}-\mathbf{x}_s)\cdot\mathbf{e}_3^s). \tag{A20}$$

Replacing s with g, the imaged point, $\mathbf{x}$, in the "geophone" local coordinate system, can be written as

$$\mathbf{x}_{Ig}' = (x_{1g}', x_{2g}', x_{3g}') = ((\mathbf{x}-\mathbf{x}_g)\cdot\mathbf{e}_1^g, 0, (\mathbf{x}-\mathbf{x}_g)\cdot\mathbf{e}_3^g). \tag{A21}$$

Then, the reflector-normal directional derivative with respect to v_0 is given (Meng, 1999), by

$$g_0(\mathbf{x}, \gamma, h) = \frac{w v_0}{4\cos\theta}\left(\frac{d_s^2(2v_{0s} + x_{3s}'w)}{\sinh(w\tau_s)v_{0s}^2(v_{0s} + wx_{3s}')^2} + \frac{d_g^2(2v_{0g} + x_{3g}'w)}{\sinh(w\tau_g)v_{0g}^2(v_{0g} + wx_{3g}')^2}\right). \tag{A22}$$

Here, d_s and d_g are the shorthand notations for

$$d_s = \sqrt{x_{1s}'^2 + x_{3s}'^2},$$

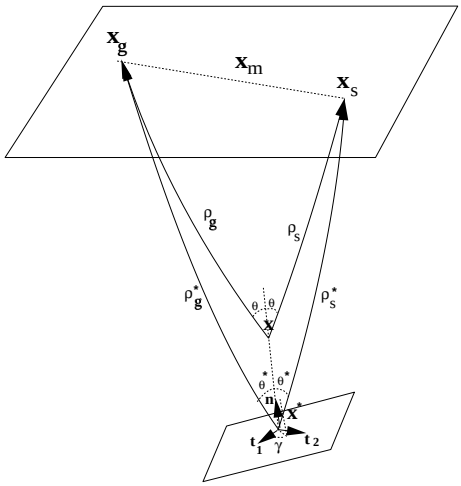

Figure A1. Ray patterns for AMVA in a constant velocity gradient background media with arbitrary reflecting subsurface. We put an $*$ to represent quantities related to the true velocity model. $\mathbf{x}^*$ is the true reflector position, ρ_s^* and ρ_g^* are the ray paths corresponding to the true velocity, c^*. Thus, ρ_s^* and ρ_g^* do not depend on azimuth γ and half offset h. ρ_s and ρ_g are the ray paths, and $\mathbf{x}(\gamma, h; c)$ is the imaged point by using data with azimuth, γ, and half offset, h, migrated with erroneous velocity, c.

and

$$d_g = \sqrt{x_{1g}'^2 + x_{3g}'^2}.$$

τ_s and τ_g are the traveltimes from the source, $\mathbf{x}_s = (x_{1s}, x_{2s}, x_{3s})$, and from the geophone, $\mathbf{x}_g = (x_{1g}, x_{2g}, x_{3g})$, to the imaged point, $\mathbf{x}$, respectively; θ is the half-opening angle (Figure A1). The reflector-normal directional derivatives with respect to velocity gradient w_k, are given by Meng (1999)

$$g_k(\mathbf{x}, \gamma, h) = \frac{v_0}{2\cos\theta}\left[\frac{w_k(\tau_s+\tau_g)}{w^2} + \left(\frac{w(x_{ks}-x_k)}{v_{0s}} - \frac{w_k}{w}\right)\frac{d_s^2(x_{3s}'w + 2v_{0s})}{2\sinh(w\tau_s)v_{0s}(x_{3s}'w+v_{0s})^2} + \left(\frac{w(x_{kg}-x_k)}{v_{0g}} - \frac{w_k}{w}\right)\frac{d_g^2(x_{3g}'w + 2v_{0g})}{2\sinh(w\tau_g)v_{0g}(x_{3g}'w+v_{0g})^2}\right], \quad k = 1,2,3. \tag{A23}$$

The above analytical formulas are numerically *unstable* for w close to zero (Meng, 1999). When this happens, the following numerically stable analytical formulas, should be used instead,

$$g_0(\mathbf{x}, \gamma, h) = \frac{v_0}{2\cos\theta}\left(\frac{d_s^2}{\tau_s v_{0s}^3} + \frac{d_g^2}{\tau_g v_{0g}^3}\right), \tag{A24}$$

and

$$g_k(\mathbf{x}, \gamma, h) = \frac{v_0}{2\cos\theta}\left[\left(2d_s(x_{ks}-x_k) + \tau_s v_{0s}x_{3s}'\right)\frac{d_s}{2\tau_s v_{0s}^3} + \left(2d_g(x_{kg}-x_k) + \tau_g v_{0g}x_{3g}'\right)\frac{d_g}{2\tau_g v_{0g}^3}\right], \quad k = 1,2,3. \tag{A25}$$

Up to this point, we have obtained a numerically *stable* analytical representation of the quantities, $g_k(\mathbf{x}, \gamma, h), k = 0, 1, 2, 3$ for arbitrary azimuth, γ, and half-offset, h. The governing equations (A8) also require that the above directional derivatives be evaluated at zero-offset. Here, the symbol $\widehat{\ }$ is used to represent the quantities at zero offset:

$$\widehat{g}_k(\mathbf{x}) = g_k(\mathbf{x}, \gamma, 0), \quad k = 0, 1, 2, 3. \tag{A26}$$

Once the reflector-normal directional derivatives, g_k's, are evaluated at different offsets, one can solve the governing equation (A8), for velocity parameter perturbations, $\delta\lambda_k$'s can be solved. A linear system solver can be used to solve such a linear system of equations (A8) for $\delta\lambda_k$, from the measured misfit $\delta L(\gamma, h)$ and the analytically evaluated directional derivatives, $\tilde{g}_k$.

Simplification of the governing equations–a horizon-based approach

A general linear system of equations, (A8), has now been obtained for velocity gradient estimation. This system of linear equations involves the measured differences in reflector-normal misfits, $\delta L(\gamma, h)$, at different offsets and/or azimuths, and the perturbations to the velocity gradients, $\delta\lambda_1 \equiv \delta v_x$, $\delta\lambda_2 \equiv \delta v_y$ and $\delta\lambda_3 \equiv \delta v_z$, and that for the top horizon velocity, $\delta\lambda_0 \equiv \delta v_0$. Since this linear system is usually poorly-conditioned, it is important to further constrain the uncertainties. Here, we adopt a horizon-based imaging approach (Wyatt, 1995). This helps to simplify the governing equations and to reduce the uncertainties. For a horizon-based approach, we represent the target layer between *top horizon* and the *base horizon*, by the functions of depth $z = z_0(x, y)$, and $z = z_1(x, y)$. In addition, for this horizon-based model representation, velocity field, $v(x, y, z)$, in the target layer is parameterized, as

$$v(x,y,z) = v_0(x,y,z_0(x,y)) + v_z(x,y)(z - z_0(x,y)), \tag{A27}$$

for $z_0(x, y) \le z < z_1(x, y)$. Here, $v_0(x, y, z_0(x, y))$ is the velocity at the top horizon, $z = z_0(x, y)$; $v_z(x, y)$ is the vertical velocity gradient in the target layer. Thus, with this representation, the x- and y-components of the velocity gradient, $v_x(x, y, z)$ and $v_y(x, y, z)$, in the target layer, can be written as

$$\frac{\partial}{\partial x}v(x,y,z) = \frac{\partial}{\partial x}v_0(x,y,z_0(x,y)) + (z - z_0(x,y))\frac{\partial}{\partial x}v_z(x,y) - n_1^0(x,y)v_z(x,y), \tag{A28}$$

and

$$\frac{\partial}{\partial y}v(x,y,z) = \frac{\partial}{\partial y}v_0(x,y,z_0(x,y)) +$$

$$(z - z_0(x,y))\frac{\partial}{\partial y}v_z(x,y) - n_2^0(x,y)v_z(x,y), \qquad \text{(A29)}$$

respectively. In other words, from equations (A28) and (A29), the perturbations to the horizontal velocity gradients, δv_x and δv_y, can be represented as

$$\delta v_x \approx \frac{\partial}{\partial x}\delta v_0 + (z - z_0)\frac{\partial}{\partial x}\delta v_z - n_1^0 \delta v_z, \qquad \text{(A30)}$$

and

$$\delta v_y \approx \frac{\partial}{\partial y}\delta v_0 + (z - z_0)\frac{\partial}{\partial y}\delta v_z - n_2^0 \delta v_z. \qquad \text{(A31)}$$

The equal sign, "=", can only be used to replace the approximate sign, "≈", when the perturbations, δv_0, δv_x, δv_y and δv_z, are infinitely small.

Since only the base horizon is imaged, $z = z_1(x,y)$ always. Replace the perturbations to the two horizontal velocity gradients, δv_x and δv_y, in the two equations (A30) and (A31) into the linear equation (A8). This reduces the system from *four* unknowns (δv_0, δv_x, δv_y and δv_z in (A8)) to a new governing equation in *two* unknowns (δv_0 and δv_z). Namely,

$$\tilde{g}_0(\gamma,h)\delta v_0 + \tilde{g}_1(\gamma,h)\left(\frac{\partial}{\partial x}\delta v_0 + \Delta z\frac{\partial}{\partial x}\delta v_z\right) +$$

$$\tilde{g}_2(\gamma,h)\left(\frac{\partial}{\partial y}\delta v_0 + \Delta z\frac{\partial}{\partial y}\delta v_z\right)$$

$$+(\tilde{g}_3(\gamma,h) - n_1^0\tilde{g}_1(\gamma,h) - n_2^0\tilde{g}_2(\gamma,h))\delta v_z = -\delta L(\gamma,h). \qquad \text{(A32)}$$

A brief analysis on equation (A32) is helpful. If a smooth solution is desired (more likely this is a requirement), the terms with partial derivatives on the left hand side in the above equation can be ignored. Then, there are only two terms remaining on the left, the terms $\tilde{g}_0\delta v_0$ and $(\tilde{g}_3 - n_1^0\tilde{g}_1 - n_2^0\tilde{g}_2)\delta v_z$. However, it is typical that these two terms compensate for each other. In other words, there is an ambiguity between the perturbation to the top horizon velocity, δv_0, and the perturbation to the vertical velocity gradient, δv_z. This typically still leaves the large linear system (A32) poorly-conditioned.

To attack this ambiguity, one should include as much information as possible to constrain the uncertainties. In particular, one approach that has been widely used is the application of regularization (Scales, 1989). Regularization can be applied to the vertical velocity gradient, δv_z, and to the perturbation to the top horizon velocity, δv_0. One way to regularize is to include the following two equations

$$\lambda_{v_z}\left(\frac{\partial^2}{\partial x^2} + \frac{\partial^2}{\partial y^2}\right)\delta v_z = 0, \qquad \text{(A33)}$$

and

$$\lambda_{v_0}\left(\frac{\partial^2}{\partial x^2} + \frac{\partial^2}{\partial y^2}\right)\delta v_0 = 0, \qquad \text{(A34)}$$

in the linear system (A32). Here, λ_{v_z} and λ_{v_0} are the regularization parameters for the vertical velocity gradient v_z and the top horizon velocity v_0, respectively.

Velocity gradient estimation with correct vertically averaged velocity

Equation (A32), as well as the regularization equations (A33) and (A34) provide us information about velocity parameter perturbations. If the data is in *good* quality and the model is reasonably *simple*, the above linear system may lead to the solution. However, if the data is in poor quality, or the model is complicated, new information may still be needed to further constrain the ambiguities.

¿From a practical point of view, one further assumption is to fix the *vertically averaged velocity*. This is reasonable if, before a velocity gradient estimation, a vertically averaged velocity has been obtained. In fact, the two-step velocity estimation algorithms introduced in Meng *et al.* (1999) provide this estimate. Thus, suppose that, the *vertically* averaged velocity, $\overline{v}(x,y)$, in the target layer,

$$\overline{v}(x,y) \equiv v(x,y,\frac{z_0(x,y) + z_1(x,y)}{2})$$

$$= v_0(x,y) + \frac{\Delta z(x,y)}{2}v_z(x,y), \qquad \text{(A35)}$$

is known before velocity gradient estimation. In other words, from equation (A35), the perturbation, δv_z, to v_z, and the perturbation, δv_0, to v_0, satisfy the following equation

$$\delta\overline{v}(x,y) \equiv \delta v_0(x,y) + \frac{\Delta z(x,y)}{2}\delta v_z(x,y) = 0, \qquad \text{(A36)}$$

or equivalently

$$\delta v_0(x,y) = -\frac{\Delta z(x,y)}{2}\delta v_z(x,y). \qquad \text{(A37)}$$

In practice, there may be other velocity constraints available. For example, if there is a (rough) estimate of the top horizon velocity, $\tilde{v}_0(x,y)$, then a constraint can be set as

$$\lambda_0\left(v_0(x,y) - \frac{\Delta z(x,y)}{2}\delta v_z(x,y) - \tilde{v}_0(x,y)\right) = 0. \qquad \text{(A38)}$$

If there is a (rough) estimate of the base horizon velocity, $\tilde{v}_1(x,y)$, then a constraint can be set as

$$\lambda_1\left(v_0(x,y) + \frac{\Delta z(x,y)}{2}\delta v_z(x,y) - \tilde{v}_1(x,y)\right) = 0. \qquad \text{(A39)}$$

Here, λ_0 and λ_1 are two parameters indicating the confidence level of the estimate of the base horizon velocity,

$\tilde{v}_0(x, y)$, and the confidence level of the estimate of the base horizon velocity, $\tilde{v}_1(x, y)$.